processes

MDPI

Article

Piperazine-Based Mixed Solvents for CO_2 Capture in Bubble-Column Scrubbers and Regeneration Heat

Pao-Chi Chen *, Jyun-Hong Jhuang and Zhong-Yi Lin

Department of Semiconductor Engineering, Lunghwa University of Science and Technology, Taoyuan City 333326, Taiwan; a0909562768@gmail.com (J.-H.J.); fawm4110@gmail.com (Z.-Y.L.)
* Correspondence: chenpc@mail2000.com.tw

Abstract: This work used piperazine (PZ) as a base solvent, blended individually with five amines, which were monoethanolamine (MEA), secondary amines (DIPAs), tertiary amines (TEAs), stereo amines (AMPs), and diethylenetriamine (DETA), to prepare mixed solvents at the desired concentrations as the test solvents. A continuous bubble-column scrubber with one stage (1 s) was first used for the test. Six parameters were selected, including the type of mixed solvent (A), the ratio of mixed solvents (B), the solvent feed rate (C), the gas flow rate (D), the concentration of the mixed solvents (E), and the liquid temperature (F), each one having five levels. Using the Taguchi experimental design, only 25 runs were required. The outcome data, such as the absorption efficiency (E_F), the absorption rate (R_A), the overall mass-transfer coefficient ($K_G a$), and the absorption factor (φ), could be determined under steady-state conditions. The optimal mixed solvents were found to be A1 (PZ + MEA) and A2 (PZ + DIPA). The parameter importance and optimal conditions for E_F, R_A, $K_G a$, and ϕ were determined separately; the verification of all optimal conditions was successful. This analysis found that the importance of the parameters was D > C > A > E > B > F, and the gas flow rate (D) was the most important factor. Subsequently, multiple-stage scrubbers were used to capture CO_2. Comparing 1 s and 3 s (three-stage scrubber), E_F, R_A, $K_G a$, and φ increased by 33%, 29%, 22%, and 38%, respectively. The desorption tests for the four optimal scrubbed solutions, including multiple stages, showed that the heat of regeneration for the three scrubbers was 3.57–8.93 GJ/t, in the temperature range of 110–130 °C, while A2 was the best solvent. Finally, the heat regeneration mechanism was also discussed in this work.

Keywords: amines; piperazine; scrubber; Taguchi; heat of regeneration

Citation: Chen, P.-C.; Jhuang, J.-H.; Lin, Z.-Y. Piperazine-Based Mixed Solvents for CO_2 Capture in Bubble-Column Scrubbers and Regeneration Heat. *Processes* **2024**, *12*, 2178. https://doi.org/10.3390/pr12102178

Academic Editor: Mariana de Mattos V. M. Souza

Received: 30 August 2024
Revised: 13 September 2024
Accepted: 3 October 2024
Published: 7 October 2024

1. Introduction

It has been internationally determined that the global average rise in temperature will not exceed 1.5 °C before 2050, compared to the levels before industrialization. However, the global surface temperature rose by nearly 1.1 °C between 2011 and 2020, accounting for 0.4 °C of the estimated 1.5 °C. The strategies for controlling CO_2 emissions ahead of 2050 have shown that the total emissions should be lowered to a value of 14 Gt CO_2 by 2050, which is a reduction of 42 Gt CO_2 compared to the current values [1]. Therefore, many methods have been proposed, including carbon capture and storage (CCS), new energy sources, including nuclear energy, and fossil fuel avoidance; among these, CCSU (carbon capture, storage, and utilization) emerges as an important tool for CO_2 reduction. This strategy has three components, including CCS, CCU, and biotechnology [2]. Amine absorption is the most widely used technique, whereby a dual-unit system combining the scrubber with the desorptor is selected, in a CO_2 concentration range of 0–20%, below 10 atm [3]. This system absorbs CO_2 whilst regenerating solvent [4–7]. The absorption of 1 ton of CO_2 by this system was internationally estimated to cost USD 52–77 in 2009 [8], with current estimates reaching USD 190 [9]. For thermal power plants, as shown in Figure 1, this value accounts for more than 1/2 of the cost of the electricity. If the cost could

be reduced to 35% of the electricity cost, this would be beneficial for the development of CCS. According to cost structure analyses, absorption operation and solvent desorption, compression, transportation, and storage account for 12%, 70%, 10%, and 8% of the cost, respectively. The literature indicates that this cost can be reduced via two methods, i.e., by improving the process [10,11] or selecting effective solvents [12,13]. Therefore, this paper first focuses on the selection of solvents and then tackles process improvement.

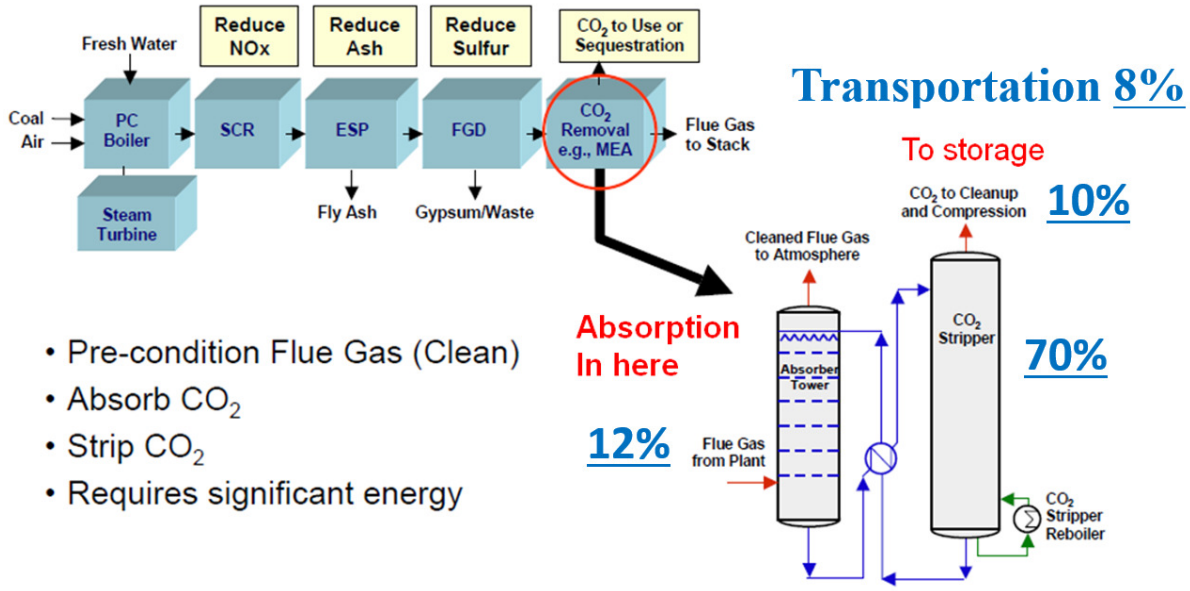

Figure 1. CO_2 capture using a double-unit process in a coal-fired plant. Red circle shows the removal of CO_2 process.

A large amount of CO_2 capture studies have been conducted in the past, focusing on solvents including amines [12,14–17], NaOH [18], K_2CO_3 [19], amino acid salt [20,21], and ionic liquids [6]. Amine solvents have been extensively studied, including single amines, such MEA, and mixed amines, mainly to explore the loading of CO_2, the reaction rates, the mass transfer coefficient, and solvent regeneration. The uses of amines, from single amines to mixed solvents, are diverse [10,22–30].

Generally speaking, amines can be classified into primary, secondary, tertiary, stereo, and cyclic amine compounds. Table 1 [31–36] shows the properties of different amines. The cyclic amine PZ (piperazine) can effectively increase absorption rates and loading [27], because it has a high reaction rate constant (53,700 $m^3/s{\cdot}kmol$ at 25 °C) and a low activation energy (33.6 kJ/mol) [6,37]. As a result, it can be used as an activator that is commonly added to MEA, DETA, DEA, MDEA, and AMP solutions to increase the CO_2 absorption rate. For example, Mondal [38] found that the loading of DEA + PZ was better than DEA + AMP, MDEA + PZ, DEA + MDEA, and TIPA + PZ when the concentration was 2–3 M. Oyenekan and Rochelle [10] used 7 M MDEA + PZ solvent to conduct CO_2 absorption and desorption tests, showing that this could save up to 22% of the energy compared to the baseline MEA. Zohi et al. [39] found that, when MDEA + PZ (5:1) was used, the absorption rate was doubled compared to the pure MDEA solvent. Moreover, Wu et al. [40] found that the efficiency of DETA + PZ was higher than that of MEA, saving 54.8% of energy. Li et al. [41] added PZ to NH_3 to study the absorption of CO_2 and found that the overall mass transfer coefficient increased with the PZ concentration. Some scholars conducted kinetic studies [31,37,42] beneficial to the widespread application of PZ. In addition to adding PZ to amines, some studies used PZ solvents for absorption and desorption tests [9].

Table 1. Performance of different solvents.

Amine	Chemical Formula	Positive Property	Negative Property	References
Primary amine	H_2N-CH_2-CH_2-OH (MEA) H_2N-CH_2-CH_2-O-CH_2-CH_2-OH (DGA)	• High absorption rate • Cheaper	• Lower in capacity • Higher in heat capacity • It cannot be used to absorb COS and CS_2 mixed gas	[31]
Secondary amine	HN-(CH_2-CH_2-H_2)$_2$ (DEPA) HN-(CH_2-C(OH)-CH_3)$_2$ (DIPA)	• It can be used to capture COS and CS_2 gasses • Lower heat capacity	• Lower loading	[32]
Tertiary amine	N-(CH_2-CH_2-OH)$_3$ (TEA) CH_3-N-(CH_2-CH_2-OH)$_2$ (MDEA)	• Higher loading • Lower heat capacity	• Lower absorption rate	[33]
Steric hindrance	HN-CH-(CH_3)$_2$-CH_2-OH (AMP)	• Higher CO_2 loading • Higher absorption rate • Good stripping property	• Higher heat capacity	[25,34]
Piperazine	$C_4H_{10}N_2$ (PZ)	• Anti-oxidation • Anti-thermal degradation • Promotes the reaction rate • Increases loading • Decreases the heat of regeneration	• Water and CO_2 absorption in air • Solubility in water	[35,36]

A good scrubbing solvent should have a high absorption capacity, a low regeneration heat, a high mass transfer rate, a high reaction rate, a low degradation rate, and low volatility [13]. PZ has these properties. In addition, thin PZ has low viscosity, toxicity, and fouling, but its cost is high. During the PZ absorption process, carbamate is first formed, followed by dicarbamate. PZ has a cyclic diamine structure that may facilitate the rapid formation of carbamates when reacting with CO_2. Theoretically, PZ can absorb two moles of CO_2 for one mole of amines [24]. So, PZ can be mixed with other amines and an appropriate scrubber under different operating conditions. Additionally, the effects on the pH values of different mixed solvents need to be studied. Also requiring consideration is the fact that PZ is loaded at higher concentrations under cold environments. For larger-scale post-combustion capture, the economic characteristics and environmental issues of the entire process are primarily determined by the choice of solvent [23]. Due to the advantages and disadvantages of PZ, the use of low-concentration PZ-based mixed solvents was considered in this study. The total concentration was less than 3 M in this work, compared to 5–7 M for the test solvents in the literature [10,13,23,24,38,40].

In our laboratory, MEA was used as a matrix with various levels of amines and a continuous scrubber to determine the optimal solvent [30]. Using outcome data, E_F, R_A, $K_G a$, and ϕ as the indicators, the results showed that MEA + PZ was the optimal solvent, followed by MEA and MEA + DIPA. Solvent regeneration showed that the ranking of the optimal solvents was MEA > (MEA + PZ) > (MEA+ DIPA). The regeneration heat load was 3.39–8.45 GJ/t-CO_2, and the value reported in the relevant literature was 2–12 GJ/t-CO_2 [30].

As discussed above, PZ can be used alone as an activator or as a mixed solvent, making its use as a matrix flexible. PZ has significant effects on CO_2 loading (α), E_F, R_A, $K_G a$, and ϕ, related to the absorption reaction. Its reaction kinetics correspond to the mode of zwitterions, similar to the primary amines and secondary amines [31,42]:

$$H_2O \rightleftharpoons H^+ + H^- \quad (1)$$

$$CO_2 + OH^- \rightleftharpoons HCO_3^- \quad (2)$$

$$CO_2 + H_2O \rightleftharpoons HCO_3^- + H^+ \quad (3)$$

$$PZ + CO_2 \underset{k_{-1}}{\overset{k_2}{\rightleftharpoons}} PZH^+COO^- \quad (4)$$

$$PZH^+COO^- + B \overset{k_B}{\rightleftharpoons} PZCOO^- + BH^+ \quad (5)$$

Equations (4) and (5) are the first-order and second-order reaction kinetics, respectively. The kinetic equation of the zwitterions in the quasi-steady state is as follows:

$$r_{PZ} = \frac{k_2[PZ][CO_2]}{1 + k_{-1}/\sum k_B[B]} \quad (6)$$

where $\sum k_B[B]$ are the alkaline components (PZ, $PZCOO^-$, PZH^+, H_2O, OH^-), which can remove protons. $k_{-1}/\sum k_B[B] = Y$ in Equation (6) determines the type I ($Y << 1$) or type II ($Y >> 1$) reaction mechanisms. However, past studies [37,42] have indicated that, as the deprotonation rate of PZ is very high, it is a type I mechanism, so Equation (6) is reduced to the following:

$$r_{PZ} = k_2[PZ][CO_2] \quad (7)$$

This is similar to the reactions of amines at all levels. Considering the mixed solvent created using PZ as the matrix and the reaction of carbonate Equations (1)–(3), the total equation is as follows:

$$r_o = k_o[CO_2] = (k_{2,PZ}[PZ] + k_{2,amine}[R_1R_2NH] + k_{H_2O}[H_2O] + k_{OH^-}[OH^-])[CO_2] \quad (8)$$

This equation is also applicable to tertiary amine $R_1R_2R_3N$, where k_{H_2O} and k_{OH^-} are the rate constants of Equations (1) and (2). According to Equation (8), the reaction rate is affected by temperature, (k_2), [PZ], [R_1R_2NH], [H_2O], [OH^-], and [CO_2], alongside various gas–liquid contact modes (scrubber).

Compared to other types of multiple-phase reactors, bubble columns are preferred for many applications. Due to their great heat and mass transfer properties, they allow for nearly isothermal operations, leading to selectivity improvements [43]. In addition, their ease of operation, internal components, simple structure, and low maintenance costs favor the making of bubble columns over fluidized beds, stirred tanks, and fixed-bed reactors [44]. Due to the complex interaction between the phases, bubble columns lead to back mixing and are hard to scale-up and design. To achieve this, the molecular size, using, for instance, different reactants, the bubble scale, such as K_Ga, and the reactor scale, including the diameter and length, need to be considered carefully. A bubble column with a multiphase reactor that can be used as a scrubber has varied applications in several fields, including in the chemical, petrochemical, biochemical, and metallurgical industry for gas–liquid and gas–liquid–solid contact or chemical reactions. In this study, a bubble-column scrubber is operated continuously, because its K_Ga and ϕ present advantages over those of packed towers and ultrahigh-speed rotating packed beds [18]. In this study, besides using a single-stage bubble column for mixed-solvent sorting, a multi-stage bubble column is tested to explore its impact on CO_2 capture, so as to improve the process. Therefore, the use of bubble columns as scrubbers is not only aimed at CO_2 capture but also at a lot of other applications.

This study is divided into two parts: the first part uses a single-stage bubble column to study the absorption of the mixed solvent with PZ as the matrix, using E_F, R_A, K_Ga, and φ as the indicators. The Taguchi method is adopted to determine the optimal mixed-solvent combination; the second part uses the solvent under optimal conditions to test a multi-stage bubble column, exploring the influence of the number of stages on various indicators. Subsequently, solvent regeneration tests are also performed for the scrubbed solutions, for both the one-stage and multi-stage column, under optimal conditions. The heating temperature is the range of 110–130 °C. The heat of vaporization, absorbed heat, and sensible heat are calculated based on the obtained data, and the heat load mechanism is further analyzed as a reference for preparing mixed solvents. According to the summary

of these two parts, the optimal mixed solvent, made using PZ as the matrix, can be obtained from the one-stage absorption test, the mixed solvent with the optimal regeneration heat duty can be obtained from the second part of this study, and the optimal solvent can thus be determined. The framework of this study is shown in Figure 2, divided into phase I and phase II, to achieve the above goals. Phase I has six factors and five levels each. The solvents can be sorted rapidly using the Taguchi experimental design.

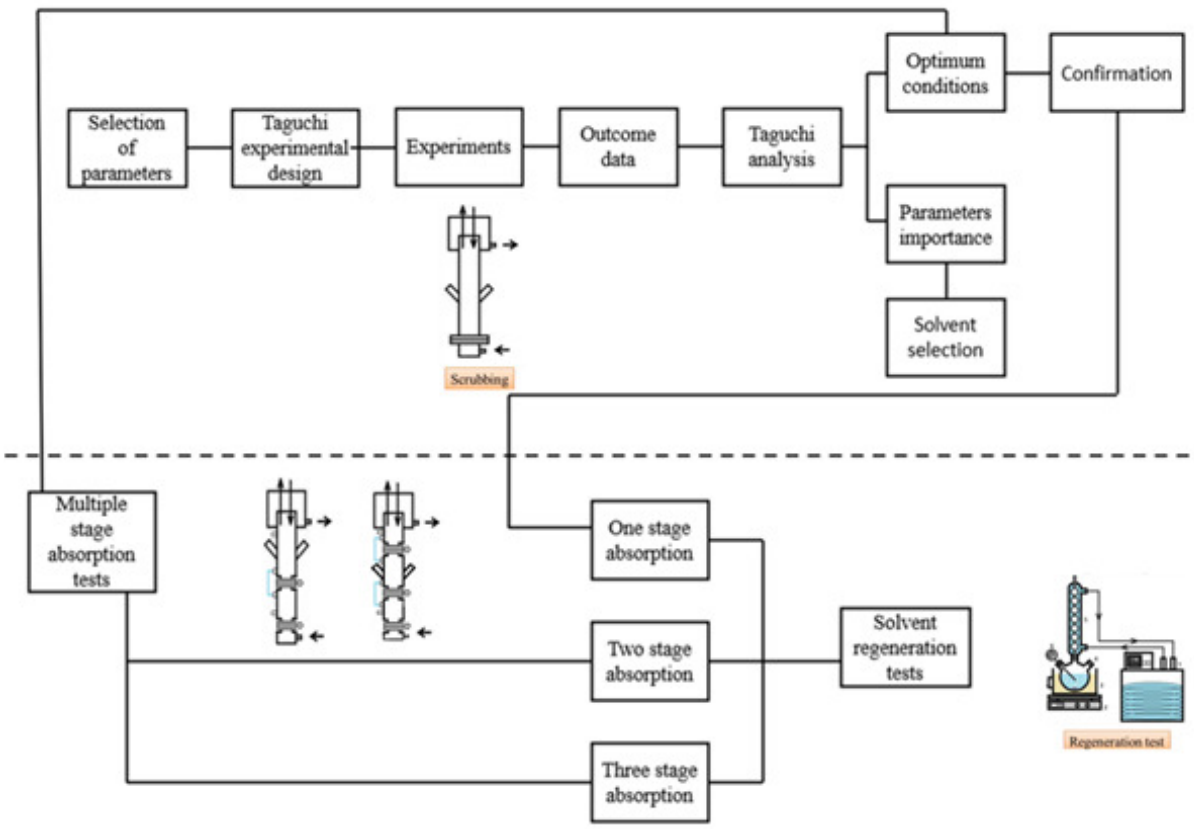

Figure 2. Framework of this study.

2. $K_G a$ and R_A Determination for Multiple-Stage Bubble-Column Scrubbers

A multiple-stage bubble-column scrubber is shown in Figure 3. In order to enhance the mixing effect, a co-current flow is utilized, as shown in the figure. We assume gas–liquid contact in one stage, remaining in equilibrium under isothermal conditions. Because of the gas–liquid contact with the co-current flow, the simulated flue gas, CO_2(A) + N_2(B), goes through the distributor, forming small bubbles and mixing with the solvent in the scrubber. The CO_2 gas from the gas film side diffuses through the interface and then into the liquid film side, being absorbed by the solvent, as shown in Figure 3b. At the interface, the CO_2 gas follows Henry's law. Using a two-film model and a multiple-plug flow model in the column [30], the multiple-stage absorption rate and overall mass transfer coefficient in the scrubber can be determined as follows:

$$-R_A = \frac{G_{AM+1}}{V_L}\left(1 - \left[\frac{1 - y_{AM+1}}{y_{AM+1}}\right]\left[\frac{y_{A1}}{1 - y_{A1}}\right]\right) \quad (9)$$

and

$$K_G a = \frac{Q_g}{V_L} \ln \frac{C_{AM}}{C_{A1}} \quad (10)$$

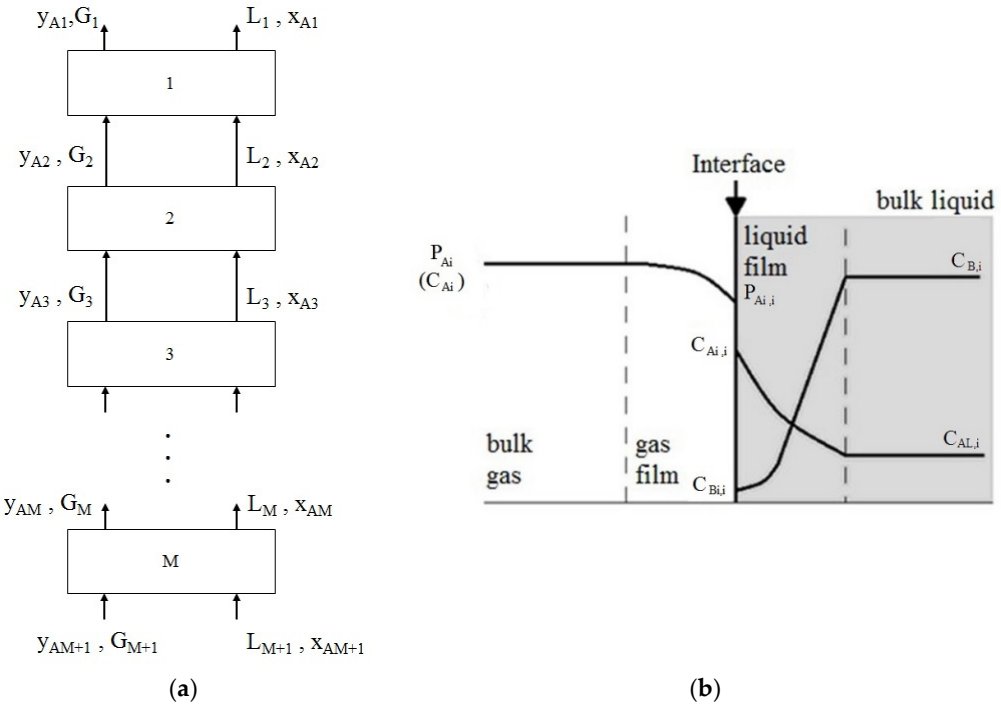

Figure 3. Absorption of CO_2 in a multiple-stage column and absorption mechanism. (**a**) Multiple-stage column; (**b**) Two-film model.

Additionally, the absorption efficient (E_F) and scrubbing factor (φ) are shown below:

$$E_F = \frac{y_{AM+1} - y_{A1}}{y_{AM+1}} \times 100\% \tag{11}$$

and

$$\phi = \frac{G_{M+1}E_F}{V_b L_{M+1}} \tag{12}$$

Here, G_i and L_i are the gas molar flow rate and the liquid molar flow rate leaving at the ith plate, respectively, while y_i and x_i represent the gas and liquid molar fractions in the ith plate, respectively. In addition, Q_g and V_L are the volume flow rate of the gas phase and the liquid volume in the column, respectively. From the measured data, indicators can be calculated using Equations (9)–(12). The derivation present in Equations (9) and (10) is shown in Supplementary Materials S1.

3. Determination of Heat of Regeneration

If one assumes no heat loss during regeneration, the heat of regeneration includes three parts, i.e., the heat of adsorption (q_{ads}), the sensitive heat (q_{sen}), and the heat of evaporation (q_{sol}), as follows:

$$\begin{aligned} q &= q_{ads} + q_{sen} + q_{sol} \\ &= \Delta H^{ad} + \frac{m_{sol} C_p \Delta T}{\Delta m_{CO_2}} + \frac{\Delta m_1}{\Delta m_{CO_2}} \Delta H^{vap} \end{aligned} \tag{13}$$

Using thermal data [45–50], the heat of regeneration, including the heat of absorption [45,48–50], the heat capacity [46], and the latent heat [51], can be determined. In Equation (12), C_p is the heat capacity of the scrubbed solutions, ΔH^{ad} is the heat of adsorption, ΔT is the temperature difference, m_{sol} is the mass of the regeneration solution at the start, Δm_{CO_2} is the mass loss of CO_2 after stripping, ΔH^{vap} is the heat of evaporation, and Δm_1 is the scrubbed solution loss during regeneration.

4. Experimental Feature

4.1. Absorption Experimental Device and Procedure

Figure 4 shows the experimental device for CO_2 absorption in the scrubber, including the bubble column, tubing pumps with a mass flow controller for the gas flow, a liquid flow meter, a pH meter, CO_2 m, a gas-heating chamber, and a liquid-cooling system [30,52]. Before starting the experiment, the desired mixed-solvent concentration was prepared using distilled water. Next, the flow rates of CO_2 (A) and N_2 (B) were adjusted with a mass flow controller at 15% of the CO_2 concentration, keeping the gas inlet temperature at 50 °C. The mixed solvent was put into the scrubber after the desired temperature and CO_2 concentration had been reached, and the experiment started. During the operation, the pH of the solution, the liquid temperature, the gas inlet temperature, the gas outlet temperature, the pressure, and the CO_2 concentration were recorded every 5 min. The liquid at the outlet was sampled for measuring the concentration of carbonate in the solution using the titration method. At the end of operation, the solvent input pump was shut, and the solution in the bubble column was withdrawn using a tubing pump to measure the volume of the liquid (V_L). Using the measured values, including P, y_{AM+1}, y_{A1}, T, and V_L, all the outcome data could be evaluated. The same procedure was applied for multiple-stage absorption. In order to compare the performance of different scrubbers, four optimal conditions, including E_F, R_A, $K_G a$, and φ, obtained from the Taguchi analysis, were used for the 1 s, 2 s, and 3 s tests.

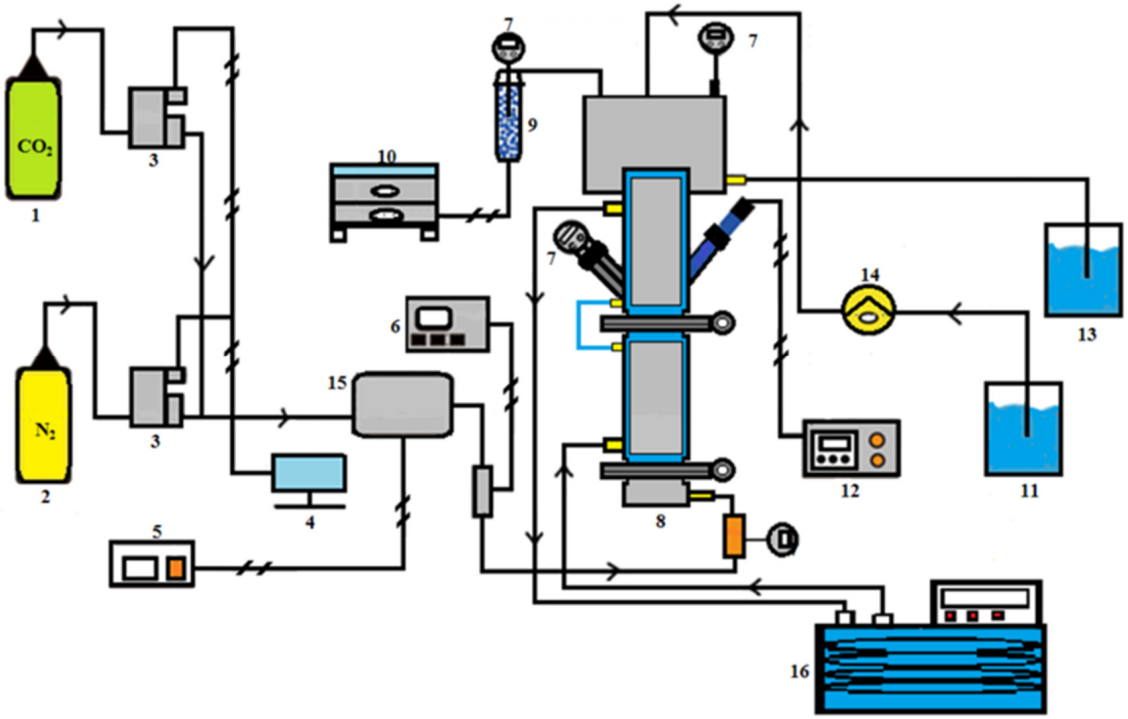

Figure 4. Device for the CO_2 absorption experiment. 1. CO_2 gas tank; 2. N_2 gas tank; 3. mass flow controller; 4. PC monitor; 5. PC; 6. pressure meter; 7. digital thermometer; 8. scrubber; 9. dryer; 10. CO_2 m; 11. solvent tank; 12. pH meter; 13. receiver tank; 14. tubing tank; 15. heater; and 16. cooler.

4.2. Taguchi Experimental Design

Six factors, including A, B, C, D, E, and F, were selected, each having five levels. According to a traditional experimental design, 15,625 runs should have been tested, leading to a long experimentation time. Using the Taguchi design, the number of experiments could be largely reduced from 15,625 to 25 runs, reducing the experimental costs by up to 99.84%. Table 2 shows the factors and levels considered in this work. According to the

Taguchi analysis, the optimal conditions and parameter importance could be determined from the outcome data, which could be estimated using the S/N ratio [21,52]:

$$\frac{S}{N} = -10 \times \log\left(\frac{1}{n} \times \sum_{i=1}^{n} \frac{1}{y_i^2}\right) \text{ the larger, the better} \quad (14)$$

$$\frac{S}{N} = -10 \times \log\left(\frac{1}{n} \times \sum_{i=1}^{n} y_i^2\right) \text{ the smaller, the better} \quad (15)$$

where n is the number of data points and y_i indicates the outcome data, including E_F, R_A, $K_G a$, and ϕ. From the S/N ratio, the optimal conditions and parameter importance can be determined using Equations (14) and (15).

Table 2. Factors and levels considered in this work.

Level	L1	L2	L3	L4	L5
Type of mixed solvent (A)	A1	A2	A3	A4	A5
Ratio of mixed solvent (B) (wt%)	10	15	20	25	30
Liquid flow rate (C) (mL/min)	150	200	250	300	350
Gas flow rate (D) (L/min)	4	6	8	10	12
Concentration of mixed solvent (E) (M)	1	1.5	2	2.5	3
Liquid temperature (F) (°C)	25	30	35	40	45

4.3. Regeneration Test

The regeneration apparatus in our work was the same as those used in a previous work [30]. This system included a ball-type condenser tube, a three-neck round flask, a heating system, and a cooling circulator, assembled as shown in Figure 2. The input cooling water temperature was set to 5 °C. Once the heating oil temperature reached the desired value (110, 120, or 130 °C) and the cooling circulator temperature was stable, the 50 g (0.05 kg) scrubbed solution was imported into the three-neck round flask, and the magnetic stirrer was switched on. The experimental time was set to sixty minutes, and the temperature change was recorded once every five minutes. When the experiment was finished, the heating controller and cooling circulator were turned off, the mass of the regenerated solution was measured, and the samples were taken for measuring CO_2 loading by the titration method. The q in Equation (12) can be determined using the measured data. Thirty-six runs were carried out.

5. Results and Discussion

5.1. Absorption Data

The absorption data, including E_F, R_A, Ka, and ϕ, could be determined under steady-state conditions, as detailed in Section 2. The data from 25 runs are summarized in Table 3, with the following ranges: 84.21–100.00%, 5.11×10^{-4}–20.20×10^{-4} mol/L·s, 0.36–1.59 s^{-1}, and 0.0434–0.2829 mol-CO_2/mol-solvent·L for E_F, R_A, $K_G a$, and ϕ, respectively. The steady-state pH values ranged from 9.98 to 11.42, depending on the operating conditions. Additionally, the γ values ranged from 0.26 to 1.95 and α ranged from 0.24 to 0.73. All the data were evaluated to identify the optimal mixed solvent.

Table 3. Absorption data for a single-stage scrubber.

No.		pH	α (mol-CO_2/mol-solvent)	E_F (%)	R_A (10^4) (mol/L·s)	$K_G a$ (1/s)	γ (-)	ϕ (mol-CO_2/L·mol-solvent)
A1	1	10.69	0.54	98.65	5.18	0.39	1.20	0.1981
	2	11.08	0.51	94.08	8.48	0.42	0.93	0.1498
	3	11.42	0.44	96.05	11.3	0.64	0.72	0.1187
	4	11.05	0.38	97.37	15.2	0.97	0.61	0.1017
	5	10.72	0.36	98.67	20.2	1.50	0.53	0.0895
A2	6	10.65	0.59	100.00	11.6	1.59	0.73	0.1223
	7	11.10	0.55	97.37	14.2	0.88	0.63	0.1056
	8	10.45	0.62	86.67	16.4	0.63	0.27	0.2719
	9	11.17	0.54	100.00	5.68	1.20	0.36	0.0613
	10	10.82	0.59	100.00	8.55	1.41	0.89	0.1504
A3	11	10.28	0.61	87.50	16.8	0.66	1.53	0.2298
	12	10.77	0.52	98.67	5.40	0.41	0.29	0.0479
	13	10.97	0.57	97.33	9.50	0.60	0.32	0.0532
	14	10.37	0.69	94.67	11.3	0.60	0.74	0.1195
	15	9.98	0.24	84.21	13.0	0.47	1.95	0.2830
A4	16	10.79	0.73	94.67	6.94	0.36	0.36	0.0584
	17	10.52	0.54	94.74	11.4	0.59	0.94	0.1526
	18	10.45	0.59	89.33	13.8	0.56	1.87	0.2829
	19	10.98	0.52	85.33	15.9	0.58	1.24	0.1789
	20	11.66	0.41	98.67	5.11	0.38	0.26	0.0434
A5	21	10.82	0.55	94.67	13.4	0.70	0.58	0.0939
	22	10.53	0.64	92.00	18.2	0.84	1.34	0.2085
	23	11.27	0.43	98.67	5.21	0.38	0.28	0.0468
	24	10.44	0.51	96.05	8.00	0.44	1.03	0.1701
	25	10.91	0.46	94.67	10.3	0.53	0.74	0.1194

5.2. Solvent Selection According to Absorption Data

Table 3 presents five types of mixed solvents: A1, A2, A3, A4, and A5. Their indicators can be compared because all the groups were subjected to the same operating conditions. Table 4 and Figure 5 show the mean values for different mixed amines. It was found that, except for $E_{F,}$ which showed minimal differences, all the other indicators exhibited significant variations. Additionally, each mixed amine was assigned a quantitative score—5, 4, 3, 2, and 1—based on the magnitude values of the indicators, as shown in Table 4 by the bold numbers within brackets. The mean values were 4, 4, 2.75, 2, and 2.25 for A1, A2, A3, A4, and A5, respectively. The results indicated that A1 (PZ + MEA) and A2 (PZ + DIPA) were the most effective mixed solvents. However, the $K_G a$ for A2 was 1.47 times that of A1, indicating that a smaller scrubber size was required when using the A2 mixed solvent.

Table 4. Mean indicators for different mixed solvents.

	E_F (%)	R_A (10^4) (mol/L·s)	$K_G a$ (1/s)	ϕ (mol-CO_2/L·mol-solvent)
A1	96.96 (5)	12.07 (5)	0.78 (4)	0.1316 (2)
A2	96.79 (4)	11.29 (4)	1.14 (5)	0.1423 (3)
A3	92.48 (1)	11.20 (3)	0.55 (2)	0.1467 (5)
A4	92.55 (2)	10.63 (1)	0.49 (1)	0.1432 (4)
A5	95.21 (3)	11.02 (2)	0.58 (3)	0.1277 (1)

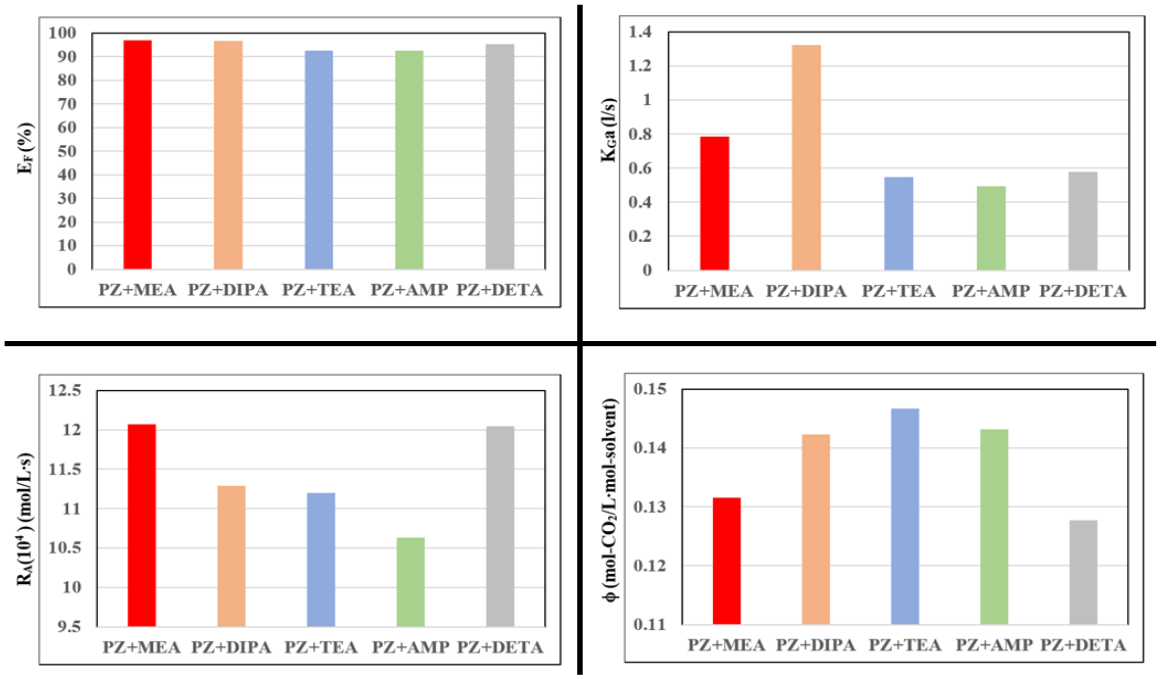

Figure 5. Comparison of indicators for different amines.

5.3. Taguchi Analysis

The S/N (signal/noise) ratios for "the larger, the better" and "the smaller, the better" could be determined using Equations (14) and (15). Table 3 shows that the maximum E_F is 100%, achieved with the A2 (PZ + DIPA) mixed solvent. Therefore, "the smaller, the better" was applied to E_F, while "the larger, the better" was used for R_A, K_Ga, and ϕ. The brackets in Table 5 highlight the maximum values for each factor. The "DELTA" value in this table indicates the difference between the maximum and minimum values of each factor, such as (A3-A1), giving 0.3968. The DELTA range was 0.1549–0.8058. For E_F, the optimal conditions and parameter sequences were A3 B3 C2 D5 E1 F3 and D > E > C > A > F > B, respectively, as shown in Table 5. The other optimal conditions and parameter sequences are detailed in Table 6. With the exception of no. 26 (E_F), the optimal conditions for no. 27–no. 29 showed that the mixed solvents A1 (no. 29) and A2 (no. 27 and no. 28) were similar to those in Section 5.2, indicating that A1 (PZ + MEA) and A2 (PZ + DIPA) were the best mixed solvents. Based on a point (0–5) analysis for six factors, as shown in Table 7, the importance of the parameters was ranked as D(4.5) > C(3.25) > A(3) > E(2.75) > B(1) > F(0.5), showing that the gas flow rate (D) was the most important factor identified in this study. However, the optimal conditions for nos. 26–29 need further verification.

Table 5. S/N ratio for E_F giving the optimal conditions and importance of the parameters.

Level	A	B	C	D	E	F
1	−39.7335	−39.5722	−39.5556	−39.9065	(−39.2978)	−39.5356
2	−39.7301	−39.5910	(−39.3407)	−39.6859	−39.3900	−39.4469
3	(−39.3367)	(−39.4376)	−39.5736	−39.6496	−39.5620	(−39.4193)
4	−39.3384	−39.5375	−39.5086	−39.3445	−39.7453	−39.5280
5	−39.5760	−39.5925	−39.7447	(−39.1007)	−39.7197	−39.7012
DELTA	0.3968	0.1549	0.4039	0.8058	0.4475	0.2819
RANK	4	6	3	1	2	5

Table 6. Optimal conditions and sequence of parameters.

	Optimal Condition	Sequence of Parameters
E_F (No. 26)	A3 B3 C2 D5 E1 F3	D > E > C > A > F > B
R_A (No. 27)	A2 B4 C5 D5 E2 F4	D > C > A > B > F > E
K_Ga (No. 28)	A2 B4 C5 D5 E4 F4	A > D > C > E > B > F
ϕ (No. 29)	A1 B4 C1 D5 E1 F1	E > D > C > A > B > F

Table 7. Factor importance analysis using a scoring analysis.

Items	A	B	C	D	E	F
E_F	2	0	3	5	4	1
R_A	3	2	4	5	0	1
K_Ga	5	1	3	4	2	0
ϕ	2	1	3	4	5	0
Mean	3	1	3.25	4.5	2.75	0.5

5.4. Verifications

To verify and compare the different columns, three types of bubble-column scrubbers were used for the tests, including one-stage (1 s), two-stage (2 s), and three-stage (3 s) bubble-column scrubbers. The operating procedure for the 2 s and 3 s scrubbers was similar to that used for 1 s. The verification results for the 1 s scrubbers, as indicated in Table 8 within the brackets, showed that E_F (minimum), R_A, K_Ga, and ϕ were 72.9%, 24.97 × 10^{-4} mol/s·L, 1.62 1/s, and 0.46 mol-CO_2/L·mole-solvent, respectively. Compared to the data from the Taguchi experiments (nos. 1–25), all the data collected under optimal conditions were successfully verified, indicating that the Taguchi experimental design used in this study was reliable. Verifications using 2 s and 3 s, also listed in Table 8 within the red brackets, were successful. Figure 6 illustrates the normalized outcome data with 1 s as the reference. It can be observed that all the values improved with an increased number of stages, demonstrating that increasing the number of stages enhances the performance of CO_2 absorption. Comparisons between the 1 s and 3 s scrubbers showed increases in the E_F, R_A, K_Ga, and ϕ by 33%, 29%, 22%, and 38%, respectively. These improvements were attributed to the increased gas–liquid contact area provided by the additional two perforated plates.

Table 8. Verifications of optimal conditions for different scrubbers.

1 s/No.	**pH**	**E_F (%)**	**R_A × 10^4 (mol/s·L)**	**K_Ga (1/s)**	**ϕ (mol-CO_2/L mol-solvent)**
1–25	9.98–11.66	86.67–100.0	5.11–20.20	0.39–1.59	0.04–0.28
26 (E_F)	9.60	(72.97)	7.85	0.23	0.19
27 (R_A)	10.80	93.33	(24.97)	1.24	0.18
28 (K_Ga)	10.92	96.00	28.45	(1.62)	0.11
29 (φ)	10.10	73.33	17.53	0.50	(0.46)
2 s/No.	**pH**	**E_F (%)**	**R_A × 10^4 (mole/s·L)**	**K_Ga (l/s)**	**ϕ(mol-CO_2/L·mol-solvent)**
30 (E_F)	10.51	(97.33)	9.38	0.606	1.372
31 (R_A)	10.95	96.00	(29.05)	1.662	0.231
32 (K_Ga)	10.86	96.00	33.92	(1.927)	0.148
33(φ)	9.80	76.00	18.89	0.567	(0.497)
3 s/No.	**pH**	**E_F (%)**	**R_A × 10^4 (mole/s·L)**	**K_Ga (l/s)**	**ϕ (mol-CO_2/L·mol-solvent)**
34 (E_F)	10.76	(97.30)	9.11	0.594	1.439
35 (R_A)	10.90	97.33	(32.16)	2.048	0.236
36 (K_Ga)	11.30	97.33	31.2	(1.977)	0.150
37(φ)	9.80	77.33	23.51	0.728	(0.636)

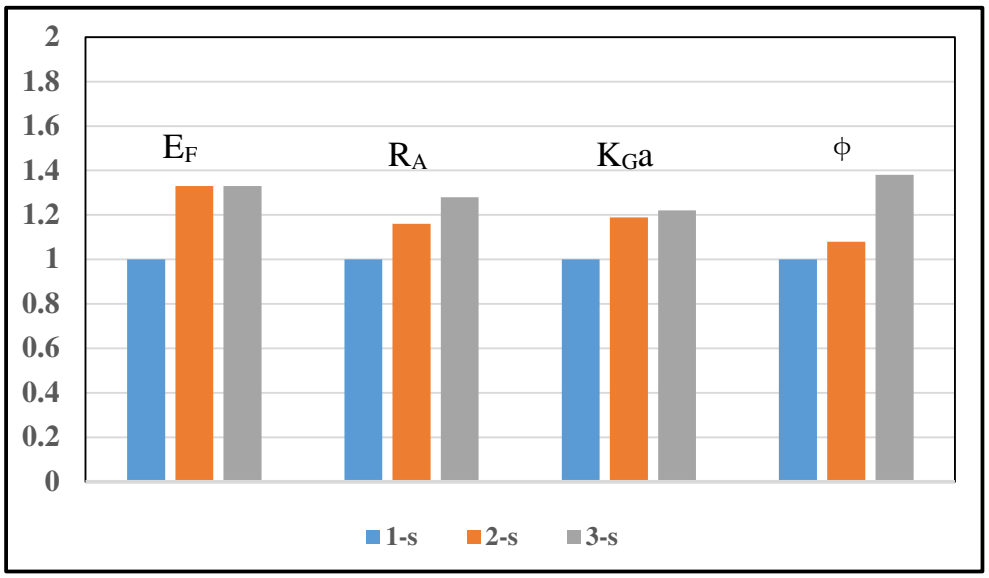

Figure 6. A plot of normalized outcome data showing the effect of the number of stages.

5.5. Heat of Regeneration

Solvent regeneration tests were conducted for four optimal conditions, nos. 26–29 (1 s), with no. 26 (1 s) used as an example. The tested temperatures were set to 110, 120, and 130 °C. The changes in the regeneration solvent temperature are shown in Figure 7. The data indicate that the temperature of the original scrubbed solution increased rapidly for 20 min and then plateaued. Using Equation (12), q_{ads}, q_{sen}, and q_{sol} were determined based on the measured and thermal data. The calculated data for the 1 s test are presented in Table 9. The total heat of regeneration ranged from 3.78 to 8.89 GJ/t, close to the range of 3.39–8.45 GJ/t reported in previous studies [30] and within the range of 2 GJ/t and 12 GJ/t reported in the literature [53–55]. All the regeneration data are listed in Supplementary Materials S2.

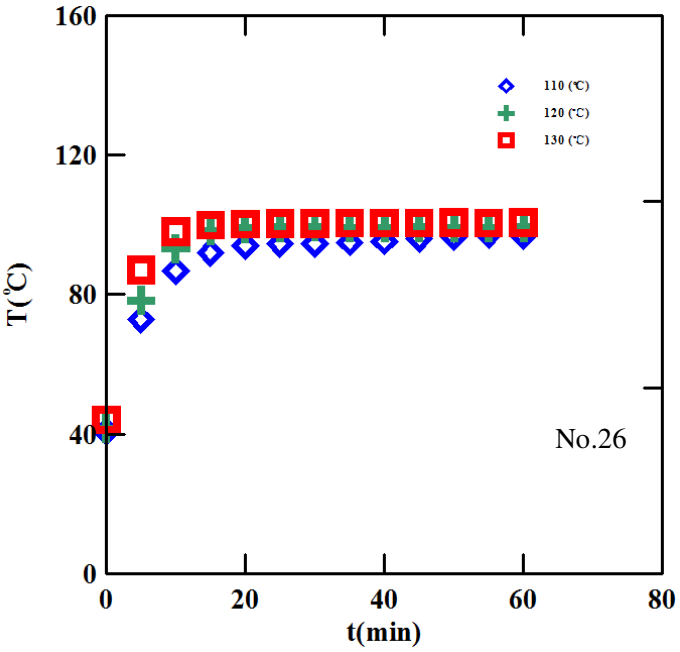

Figure 7. Regeneration temperature changes with time under different conditions.

Table 9. Heat of regeneration for 1 s at different scrubber temperatures.

1 s	T (°C)	q_{sen} (GJ/ton)	q_{sol} (GJ/ton)	q_{ads} (GJ/ton)	q (GJ/ton)
E_F (No. 26) (PZ + TEA)	110	0.56 (0.148)	2.00 (0.529)	1.22 (0.323)	3.78
	120	1.03 (0.155)	4.41 (0.662)	1.22 (0.183)	6.66
	130	1.57 (0.177)	6.10 (0.686)	1.22 (0.137)	8.89
R_A (No. 27) (PZ + DIPA)	110	0.72 (0.134)	2.92 (0.544)	1.73 (0.322)	5.37
	120	0.93 (0.135)	4.23 (0.614)	1.73 (0.251)	6.89
	130	1.10 (0.140)	4.98 (0.638)	1.73 (0.222)	7.81
K_Ga (No. 28) (PZ + DIPA)	110	0.56 (0.101)	3.24 (0.586)	1.73 (0.313)	5.53
	120	0.87 (0.148)	3.32 (0.560)	1.73 (0.292)	5.93
	130	1.20 (0.150)	5.06 (0.633)	1.73 (0.217)	7.99
ϕ (No. 29) (PZ + MEA)	110	0.69 (0.130)	3.24 (0.620)	1.31 (0.250)	5.23
	120	0.92 (0.151)	3.88 (0.635)	1.31 (0.214)	6.11
	130	1.06 (0.125)	6.13 (0.721)	1.31 (0.154)	8.50

5.5.1. Regeneration Mechanism

The individual energy estimations (1 s) for q_{sen}, $q_{sol,}$ and q_{ads} were 0.56–1.57 GJ/t, 2.0–6.13 GJ/t, and 1.22–1.73 GJ/t, respectively. The fractions (*Fs*) of the individual required energies ranged from 0.101 to 0.151, 0.529 to 0.721, and 0.137 to 0.342 for q_{sen}, q_{sol}, and q_{ads}, respectively. According to the 1 s solvent regeneration test, the heat regeneration sequence at three temperature averages was no. 26 (6.44) < no. 28 (6.48) < no. 29 (6.61) < no. 27 (6.69), with slightly differences among them. Moreover, the heat of regeneration of different scrubbers increased with an increase in the regeneration temperature, as shown in Figure 8, which was similar to that reported in the literature [21,22] when the loading was higher than 0.4. To explore the regeneration mechanism, Figure 9 plots the total heat of regeneration against the fractions of individual energies (Fs). The values ranges were 0.10–0.20 (Figure 9a), 0.40–0.70 (Figure 9b), and 0.20–0.40 (Figure 9c) for q_{sen}, q_{sol}, and q_{ads}, respectively. This shows that the fraction of q_{sol} was the dominating factor compared to q_{sen} and q_{sol}. Additionally, the fraction of q_{sol} increased with an increase in q, while the fraction of q_{ads} increased with a decrease in q.

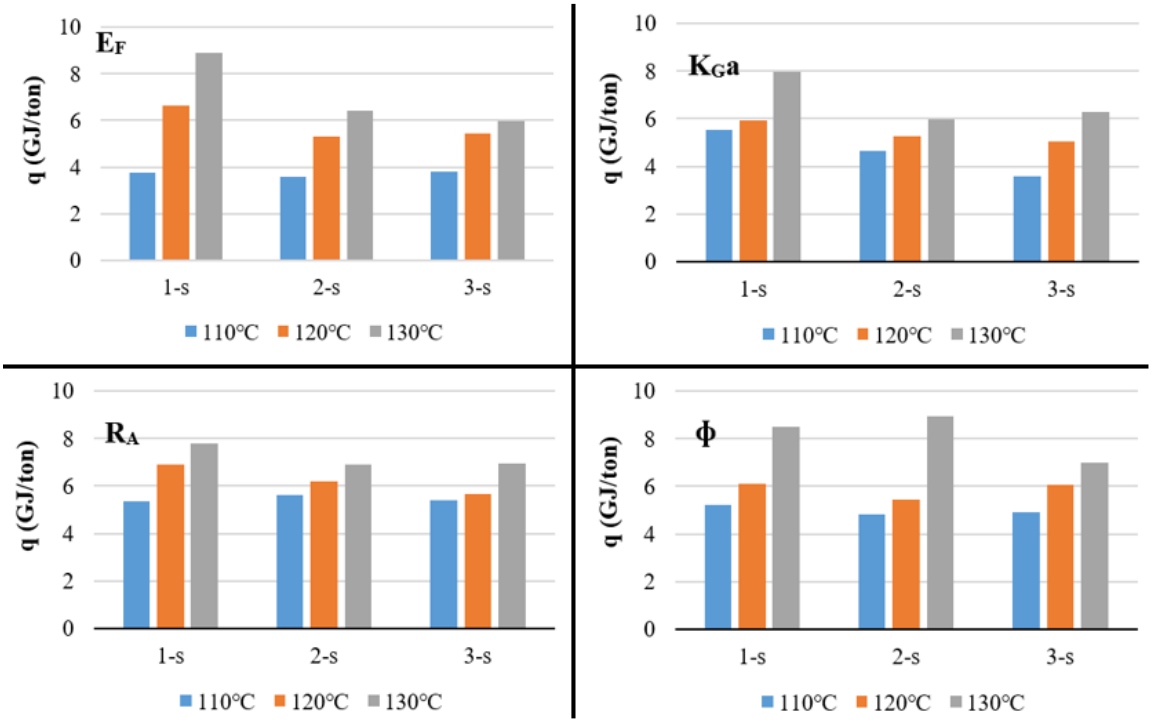

Figure 8. Heat of regeneration for different scrubbed solutions.

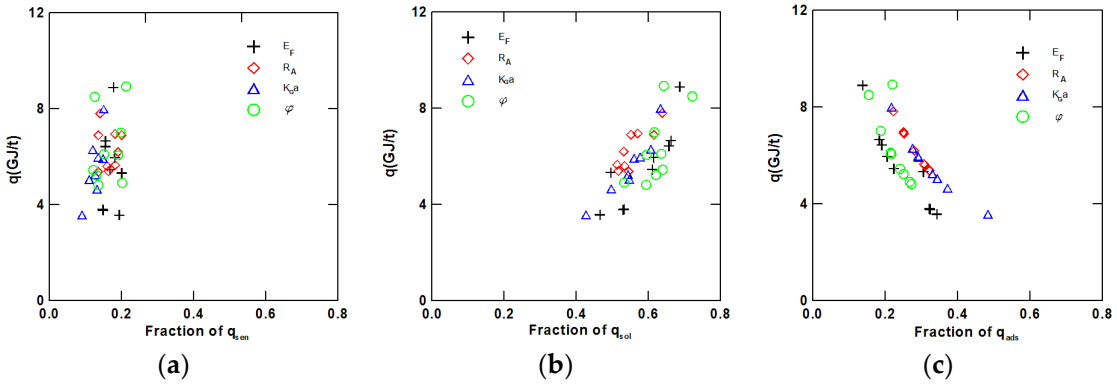

Figure 9. Analysis of heat of regeneration. (**a**) Fraction of sensitive heat; (**b**) fraction of heat of evaporation; (**c**) fraction of heat of adsorption.

5.5.2. Selection of Solvent

Following the discussion in the previous section, there are two major ways to decrease q: selecting a solvent with a lower heat of absorption (such as no. 26) or using a higher-concentration solvent to reduce the heat of evaporation (such as 1.5 M for no. 27 and 2.5 M for no. 28), alongside those reported in the literature [14,16]. A2 and A3 were the selected solvents in this study. Additionally, a higher α, which is related to the pH, t, and C_t, can control the heat of regeneration. A regression analysis of α is required and can be expressed as follows:

$$\alpha = \beta(\mathrm{pH})^{a} t^{b} C_t^{d} \quad (16)$$

The regression results for different mixed solvents are shown in Table 10. The R^2 values for different mixed solvents are also presented in this table. The regressions are considered reliable because the R^2 values exceed 0.6 in all cases. It can be observed that α increases when the conditions involve a lower pH, a lower t, or a higher C_t for most cases. Alternatively, the heat of regeneration (q) can be expressed in terms of the solution pH, the

generation temperature (t), and the loading difference ($\Delta\alpha$). The regression result for all regeneration data (36 data points) becomes as follows:

$$q = 4.2023 \times 10^{-2} \mathrm{pH}^{-1.4297} t^{1.4898} (\Delta\alpha)^{-0.3419} \quad (17)$$

Table 10. Parameters of the correlation equations in Equation (15).

Solvent	a	b	d	β	R^2
A1	−1.3177	−3.8818	1.6903	3.286×10^6	0.9874
A2	−1.9763	−0.001270	−0.001381	64.393	0.9654
A3	−0.4644	0.5403	0.9654	0.1241	0.6652
A4	−5.8458	−0.006955	0.4151	4.961×10^5	0.9665
A5	−3.4909	−0.1259	0.1789	2.730×10^3	0.9656

The R square in our study was found to be 0.7814, and the deviation between the measured data and the calculated data is shown in Figure 10. The smaller deviation shows that the result was reliable. The regression results state that q attenuates when conditions involve a higher pH, a lower t, or a higher $\Delta\alpha$.

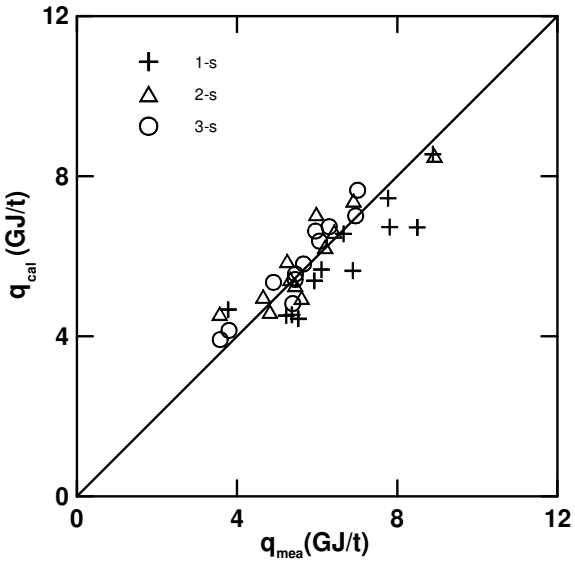

Figure 10. Plot of q_{cal} versus q_{mea}, showing the reliability of regression analysis.

6. Conclusions

A lab-scale continuous bubble-column scrubber for CO_2 capture was effectively used to assess the performance of PZ-based mixed solvents from absorption and heat regeneration data. According to the Taguchi analysis, the parameters' importance was ranked as D > C > A > E > B > F, indicating that the gas flow rate (D) was the most important factor, while the liquid flow rate (C) came second. The priority sequence of the mixed solvents was A1 = A2 > A3 > A5 > A4. The absorption efficiency could be controlled within values greater than 90% when γ was in the range of 0.27–1.87. The verification of 1 s demonstrated that all the data collected under optimal conditions were successfully verified, indicating the reliability of the Taguchi experimental design. Additionally, the verifications using 2 s and 3 s were also successful, indicating that all performance metrics improved with an increase in the number of stages. This suggests that CO_2 capture performance can be enhanced by increasing the number of stages. The heat of regeneration for the three scrubbers ranged from 3.57 to 8.93 GJ/t, depending on the operating conditions. This shows that the fraction of q_{sol} was the dominating factor, compared to q_{sen} and q_{ads}. Additionally, α could be controlled by adjusting the pH, the t, and the C_t, while q could be reduced when conditions involved a higher pH, a lower t, or a higher $\Delta\ \alpha$. Based on our CO_2 capture

study and heat regeneration tests, A2 (PZ + DIPA) is the preferred choice. The optimal conditions were identified to be B = 25%, C = 350 mL/min, D = 12 L/min, E = 1.5–2.5 M, and F = 40 °C. Finally, the results showed that the Taguchi method is a quick screening method for obtaining the optimal mixed solvent. The above results regarding CO_2 capture can also be used as a reference in several field, including in the chemical, petrochemical, biochemical, and metallurgical industry, for gas–liquid and gas–liquid–solid contact or chemical reactions.

Supplementary Materials: The following supporting information can be downloaded at: https://www.mdpi.com/article/10.3390/pr12102178/s1, Figure S1: A mutiple-tube mass balance model; Table S1: CO2 loading data before and after regenerations; Table S2: Heat of regeneration data obtained according to E_F optimum condition; Table S3: Heat of regeneration data obtained according to R_A optimum condition; Table S4: Heat of regeneration data obtained according to KGa optimum condition; Table S5: Heat of regeneration data obtained according to ϕ optimum condition.

Author Contributions: Methodology, P.-C.C.; software, J.-H.J. and Z.-Y.L.; validation, J.-H.J.; formal analysis, P.-C.C. and Z.-Y.L.; investigation, Z.-Y.L.; resources, J.-H.J. and Z.-Y.L.; data curation, J.-H.J.; writing—original draft, J.-H.J.; writing—review and editing, P.-C.C.; project administration, P.-C.C.; funding acquisition, P.-C.C. All authors have read and agreed to the published version of the manuscript.

Funding: This research was funded by Overseas Chinese Environmental Engineers & Scientists Association (AOI-3).

Data Availability Statement: The original contributions presented in the study are included in the article, further inquiries can be directed to the corresponding author.

Conflicts of Interest: The authors declare no conflicts of interest.

References

1. Masson-Delmotte, V.; Zhai, P.; Pörtner, H.-O.; Roberts, D.; Skea, J.; Shukla, P.R.; Pirani, A.; Moufouma-Okia, W.; Péan, C.; Pidcock, R.; et al. (Eds.) *Special Report on Global Warming of 1.5 °C (SR15)*; Intergovernmental Panel on Climate Change (IPCC): Geneva, Switzerland, 2018.
2. Gabrielli, P.; Poluzzi, A.; Kramer, G.J.; Spiers, C.; Mazzotti, M.; Gazzani, M. Seasonal energy storage for zero-emissions multi-energy systems via underground hydrogen storage. *Renew. Sustain. Energy Rev.* **2020**, *121*, 109629. [CrossRef]
3. Han, K.; Ahn, C.K.; Lee, M.S. Performance of an ammonia-based CO_2 Capture pilot facility in iron and steel industry. *Int. J. Greenh. Gas Control* **2014**, *27*, 239–246. [CrossRef]
4. Khan, U.; Ogbaga, C.C.; Omolabake Abiodun, K.O.; Adeleke, A.A.; Ikubanni, P.P.; Okoye, P.U.; Okolie, J.A. Assessing absorption-based CO_2 capture: Research progress and techno-economic assessment overview. *Carbon Capture Sci. Technol.* **2023**, *8*, 100165. [CrossRef]
5. Mangalapally, H.P.; Notz, R.; Hoch, S.; Asprion, N.; Sieder, G.; Garcia, H.; Hasse, H. Pilot plant experimental studies of post combustion CO_2 capture by reactive absorption with MEA and new solvents. *Energy Procedia* **2009**, *1*, 963–970. [CrossRef]
6. Yu, C.H.; Huang, C.H.; Tan, C.S. A Review of CO_2 Capture by absorption and adsorption. *Aerosol Air Qual. Res.* **2012**, *12*, 745–769. [CrossRef]
7. Oexmann, J.; Kather, A. Minimising the regeneration heat duty of post-combustion CO_2 capture by wet chemical absorption: The misguided focus on low heat of absorption solvents. *Inter. Greenh. Gas Control* **2010**, *4*, 36–43. [CrossRef]
8. Rochelle, G.T. Amine scrubbing for CO_2 capture. *Science* **2009**, *325*, 1652–1654. [CrossRef]
9. Babu, A.S.; Rochelle, G.T. Cost-effective stripper designs for CO_2 capture on a 460 MW NGCC using piperazine. *Carbon Capture Sci. Technol.* **2024**, *11*, 100196. [CrossRef]
10. Oyenekan, B.A.; Rochelle, G.A. Alternative stripper configurations for CO_2 capture by aqueous solution amines. *AIChE J.* **2007**, *53*, 3144–3154. [CrossRef]
11. Feron, P.H.M. The potential for improvement of the energy performance of pulverized coal fired power stations with post-combustion capture of carbon dioxide. *Energy Procedia* **2009**, *1*, 1067–1074. [CrossRef]
12. Salazar, J.; Diwekar, U.; Joback, K.; Berger, A.H.; Bhown, A.S. Solvent selection for post-combustion CO_2 capture. *Energy Procedia* **2013**, *37*, 257–264. [CrossRef]
13. Mathia, P.M.; Reddy, S.; Smith, A.; Afshar, K. Aguide to evaluate solvents and processes for post-combustion CO_2 capture. *Energy Procedia* **2013**, *37*, 1863–1870. [CrossRef]
14. Stec, M.; Tatarczuk, A.; Cław-Solny, L.W.; Krotki, A.; Spietz, T.; Wilk, A.; Spiewak, D. Demonstration of a post-combustion carbon capture pilot plant using amine-based solvents at the Łaziska Power Plant in Poland. *Clean Techn Env. Policy* **2016**, *18*, 151–160. [CrossRef]

15. Kim, I.; Hoff, K.A.; Mejdell, T. Heat of absorption of CO_2 with aqueous solutions of MEA: New experimental data. *Energy Procedia* **2014**, *63*, 1446–1455. [CrossRef]
16. Hack, J.; Maeda, N.; Meier, D.M. Review on CO_2 Capture Using Amine-Functionalized Materials. *ACS Omega.* **2022**, *7*, 39520–39530. [CrossRef]
17. Lopez, A.B.; La Rubia, M.D.; Navaza, J.M.; Pacheco, R.; Gomez-Dıaz, D. Characterization of MIPA and DIPA aqueous solutions in relation to absorption, speciation and degradation. *J. Ind. Eng. Chem.* **2015**, *21*, 428–435. [CrossRef]
18. Choi, B.K.; Kim, S.M.; Lee, J.S.; Park, Y.C.; Chun, D.H.; Shin, H.Y.; Sung, H.J.; Min, B.M.; Moon, J.H. Effect of blending ratio and temperature on CO_2 solubility in blended aqueous solution of monoethanolamine and 2-amino-2-methyl-propanol: Experimental and modeling study using the electrolyte nonrandom two-liquid model. *ACS Omega* **2020**, *5*, 28738–28748. [CrossRef]
19. Chen, P.C. Absorption of carbon dioxide in a bubble-column scrubber. In *Greenhouse Gases—Capturing, Utilization and Reduction*; InTech: Houston, TX, USA, 2012; Chapter 5; pp. 95–116. [CrossRef]
20. Borhani, T.N.G.; Azarpour, A.; Akbari, V.; Alwi, S.R.W.; Manan, Z.A. CO_2 capture with potassium carbonate solutions: A state-of-the-art review. *Int. L J. Greenh. Gas Control* **2015**, *41*, 142–162. [CrossRef]
21. Kumar, P.S.; Hogendoorn, J.A.; Versteeg, G.F.; Feron, P.H.M. Kinetics of the reaction of CO_2 with aqueous potassium salt of Taurine and Glycine. *AIChE J.* **2003**, *49*, 203–213. [CrossRef]
22. Chen, P.C.; Lin, S.Z. Optimization in the absorption and desorption of CO_2 using sodium glycinate solution. *Appl. Sci.* **2018**, *8*, 2041. [CrossRef]
23. Aroonwilas, A.; Veawab, A. Integration of CO2 capture unit using blended MEA-AMP solution into coal-fired power plants. *Energy Procedia* **2009**, *1*, 4315–4321. [CrossRef]
24. Dash, S.K.; Samanta, A.N.; Bandyopadhyay, S.S. Simulation and parametric study of post combustion CO_2 capture process using (AMP+PZ) blended solvent. *Int. J. Greenh. Gas Control* **2014**, *21*, 130–139. [CrossRef]
25. Artanto, Y.; Jansen, J.; Pearson, P.; Puxty, G.; Cottrell, A.; Meuleman, E.; Feron, P. Pilot-scale evaluation of AMP/PZ to capture CO_2 from flue gas of Australain brown coal-fired power station. *Inter. Greenh. Gas Control* **2014**, *20*, 189–195. [CrossRef]
26. Neveux, T.; Moullec, Y.L.; Corriou, J.P.; Favre, E. Energy performance of CO_2 capture process: Interaction between process design and solvent. *Chem. Eng. Trans.* **2013**, *35*, 337–342. [CrossRef]
27. Lai, Q.; Kong, L.; Gong, W.; Russell, A.G.; Fa, M. Low-energy-consumption and environmentally friendly CO_2 capture via blending alcohols into amine solution. *Appl. Energy* **2019**, *254*, 113696. [CrossRef]
28. Lin, P.H.; Wong, D.S.H. Carbon dioxide capture and regeneration with amine/alcohol/water blends. *Inter. Greenh. Gas Control* **2014**, *26*, 69–75. [CrossRef]
29. Wu, S.H.; Caparanga, A.R.; Leron, R.B.; Li, M.H. Vapropressures of aqueous blend-amine solutions containing (TEA/AMP/MDEA)+(DEA/MEA/PZ) at temperatures (303.15–343.15)K. *Exp. Therm. Fluid Sci.* **2013**, *48*, 1–7. [CrossRef]
30. Li, T.; Keener, T.C. A review: Desorption of CO_2 from rich solutions in chemical absorption processes. *Int. Greenh. Gas Control* **2016**, *51*, 290–304. [CrossRef]
31. Chen, P.C.; Jhuang, J.H.; Wu, T.W.; Yang, C.Y.; Wang, K.Y.; Chen, C.M. Capture of CO_2 Using Mixed Amines and Solvent Regeneration in A Lab-scale Continuous Bubble-column Scrubber. *Appl. Sci.* **2023**, *13*, 7321. [CrossRef]
32. Vaidya, P.D.; Kenig, E.Y. CO_2-alkanomine reaction kinetics: A review of recent work. *Chem. Eng. Technol.* **2007**, *30*, 1467–1474. [CrossRef]
33. Adeosun, A.; Hadri, N.E.; Goetheer, E.; Abu-Zahra, M.R.M. Absorption of CO_2 by Amine Blends Solution: An Experimental Evaluation. *Int. J. Eng. Sci.* **2013**, *3*, 12–23. [CrossRef]
34. Xiao, J.; Li, C.C.; Li, M.H. Kinetics of absorption of carbon dioxide into aqueous solutions of 2-amino-2-methyl-1-propanol+monoethanolamin. *Chem. Eng. Sci.* **2000**, *55*, 161–175. [CrossRef]
35. Choi, W.J.; Seo, J.B.; Jang, S.Y.; Jung, J.H.; Oh, K.J. Removal characteristics of CO2 using aqueous MEA/AMP solutions in the absorption and regeneration process. *J. Environ. Sci.* **2009**, *21*, 907–913. [CrossRef]
36. Van Wagener, D.H.; Rochelle, G.T. Stripper configurations for CO_2 capture by aqueous monoethanolamine. *Chem. Eng. Res. Des.* **2011**, *89*, 1639–1646. [CrossRef]
37. Mazari, S.A.; Ali, B.S.; Jan, B.M.; Saeed, I.M. Degradation study of piperazine, its blends and structural analogs for CO_2 capture: A review. *Inter. Greenh. Gas Control.* **2014**, *31*, 214–228. [CrossRef]
38. Bishnoi, S.; Rochelle, G.T. Absorption of carbon dioxide into aqueous piperazine: Reaction kinetics, mass transfer and solubility. *Chem. Eng. Sci.* **2000**, *55*, 5531–5543. [CrossRef]
39. Mondal, M.K. Absorption of carbon dioxide into a mixed aqueous solution of diethanolamine and piperazine. *IJCT* **2010**, *17*, 431–435. [CrossRef]
40. Zoghi, A.T.; Feyzi, F.; Zarrinpashneh, S. Experimental investigation on the effect of addition of amine activators to aqueous solutions of *N*-methyldiethanolamine on the rate of carbon dioxide absorption. *Inter. Greenh. Gas Control* **2012**, *7*, 12–19. [CrossRef]
41. Wu, T.W.; Hung, Y.T.; Chen, M.T.; Tan, C.S. CO_2 capture from natural gas power plants by aqueous PZ/DETA in rotating packed bed. *Sep. Purif. Technol.* **2017**, *186*, 309–317. [CrossRef]
42. Li, L.; Conway, W.; Puxty, G.; Burns, R.; Clifford, S. The effect of paerazinr (PZ) on CO_2 absorption kinetics into aqueous ammonia solutions at 25 °C. *Inter. Greenh. Gas Control* **2015**, *36*, 135–143. [CrossRef]
43. Derks, P.W.J.; Kleigeld, T.; Van Aken, C.; Hogendoorn, J.A.; Versteeg, G.F. Kinetics of absorption of carbon dioxide in aqueous 533 piperazine solutions. *Chem. Eng. Sci.* **2006**, *61*, 6837–6854. [CrossRef]

44. Shetty, S.A.; Kan Tak, M.V.; Kelkar, B.G. Gas-phase backmixing in bubble-column reactors. *AIChE J.* **1992**, *38*, 1013–1026. [CrossRef]
45. Youssef, A.A.; Al-Dahhan, M.H.; Dudukovic, M.P. Bubble columns with internals: A review. *Inter. J. Chem. Reac. Eng.* **2013**, *11*, 169–223. [CrossRef]
46. Wanderley, R.R.; Ponce, G.J.C.; Knuutila, H.K. Solubility and heat of absorption of CO_2 into diisopropylamine and N,N-diethylethanolamine mixed with organic solvents. *Energy Fuels* **2020**, *34*, 8552–8561. [CrossRef]
47. Chiu, L.F.; Li, M.H. Heat capacity of alkanolamine aqueous solutions. *J. Chem. Eng. Data* **1999**, *44*, 1396–1401. [CrossRef]
48. Eller, K.; Henkes, E. *Ullman's Encyclopedia of Industrial Chemistry*, 7th ed.; John Wiley & Sons: Hoboken, NJ, USA, 2005.
49. Elhajj, J.; Al-Hindi, M.; Azizi, F. A Review of the absorption and desorption processes of carbon dioxide in water systems. *Ind. Eng. Chem. Res.* **2014**, *53*, 2–22. [CrossRef]
50. Ojala, M.S.; Serrano, N.F.; Uusi-Kyyny, P.; Alopaeus, V. Comparative study: Absorption enthalpy of carbon dioxide into aqueous diisopropanolamine and monoethanolamine solutions and densities of the carbonated amine solutions. *Fluid Phase Equilibria* **2014**, *25*, 85–95. [CrossRef]
51. Kim, E.K.; Yun, S.H.; Xhoi, J.H.; Nam, S.C.; Park, S.Y.; Jeong, S.K.; Yoon, Y.I. Comparison of CO_2 absorption characteristics of aqueous solutions of diamines: Absorption capacity, specific heat capacity, and heat of absorption. *Energy Fuels* **2015**, *29*, 2582–2590. [CrossRef]
52. Mirzaei, S.; Shamiri, A.; Aroua, M.K. A review of different solvents, mass transfer, and hydrodynamics for postcombustion CO_2 capture. *Rev. Chem. Eng.* **2015**, *31*, 521–561. [CrossRef]
53. Chen, P.C.; Chou, P.H.; Lin, S.Z.; Chen, H.W. Capturing CO_2 by using a microalgae culture recycle solution. *Chem. Eng. Tech.* **2017**, *40*, 2274–2282. [CrossRef]
54. Zhang, X.; Fu, K.; Liang, Z.; Yang, Z.; Rongwong, W.; Na, Y. Experimental studies of regeneration heat duty for CO_2 desorption from aqueous DETA solution in a randomly packed column. *Energy Procedia* **2014**, *63*, 1497–1503. [CrossRef]
55. Mangalapally, H.P.; Hasse, H. Pilot plant experiments for post combustion carbon dioxide capture by reactive absorption with novel solvents. *Energy Procedia* **2011**, *4*, 1–8. [CrossRef]